EVALUATION OF THE PLASTIC ZONE SIZE AT THE FRONT OF A FATIGUE CRACK BY X-RAY FRACTOGRAPHY

A. BIGNONNET*,
J.L. LEBRUN**, B. GUIMARD**

X-Ray fractography may be used to determine the plastic zone size of a fatigue crack, from the fracture surface. The plastic zone size is determined by stresses measurements, and peak breadth evolution. Comparison of experimental results and analytical solution show a good agreement.

X-Ray fractography, allows to measure in plane strain conditions, plastic zone size as small as 50 μm.

INTRODUCTION

The X-Ray fractography technique presented in this study is developed to provide a new method of investigation of the fatigue crack plastic zone. Early measurements by X-Ray fractography performed by Tanaka and Hatanaka (1) and Kurebayashi et al (2), in high strength and mild steels, illustrate the interest of the technique. The local plastic deformation, that occurs at a fatigue crack tip, leaves residual stresses and deformations on the fracture surface. The study of the material deformation and work hardening through the displacement and broadening of X-Ray diffraction peaks, gives useful information on the fatigue process. In depth measurements allow the determination of fatigue crack plastic zone. An encouraging comparison between experimental values and analytical solutions shows the adequacy of the method for fatigue fracture study.

MATERIAL AND FATIGUE TESTS

Material and specimens

The material investigated is a quenched and tempered structural steel E 550 in 20 mm thick plate. This material, quenched after rolling and tempered at 625°C for 20 mn, presents a tempered martensitic microstructure. Chemical composition and mechanical properties are in table 1a and 1b.

C	Mn	Si	S	P	Nb
0.145	1.410	0.360	0.001	0.020	0.018

Table 1a - Chemical analysis (weight %)

---

*IRSID, Saint-Germain-en-Laye - France
**ENSAM, Paris - France

σ_{ys} (MPa)	UTS (MPa)	Elong. (%)	Red. in area (%)	σ'_{ys} (MPa)	Kcv (- 40°c) (J/cm^2)
570	720	20	77	400	67

Table 1b - Mechanical properties

The specimens used for the fatigue tests are of CT type, W = 80 mm, B = 18 mm, machined in the LT orientation.

Fatigue testing

Fatigue tests were carried out on an electro-servohydraulic testing machine, operating under load control. Each test was performed with a constant amplitude load (sine wave) and the influence of two parameters, stress ration (R) and test frequency (f) was investigated. Two R ratios were chosen : R = 0.1 and 0.7, in each case two different tests were performed with different load signal frequencies, typically f = 65 Hz and 7 Hz. The following table indicates the fatigue tests conditions in each cases.

Referenced as	A	B	C	D
Stress ratio R	0.1	0.1	0.7	0.7
Load frequency (Hz)	65	7	65	7
ΔK initial (MPa $\sqrt{m}$)	9.5	9.5	6.0	6.0

For the "65 Hz test", when the crack growth rate was higher than $\sim 2 \times 10^{-8}$ m/c the load signal frequency was lowered to 35 Hz.

Table 2 - Fatigue test conditions

The crack length was measured with a travelling microscope (x 40). Crack closure measurements were obtained, using a clip-on gauge (operating frequency up to 200 Hz without distorsion) or back face strain gauge (full bridge with 350 Ω gauges) as proposed by Kikuwa et al (3). Both techniques gave exactly the same results. A numerical oscilloscope allowed measurement at the test frequency. The environment was laboratory air. Continuous records of temperature and relative humidity close to the specimen showed that for all the tests the temperature was 22°C and the relative humidity was 25 ± 5 %.

X-RAY FRACTOGRAPHY TECHNIQUE

These experiments are mainly based on residual stress measurements by X Ray diffraction. The technique is well known and has recently been improved both on theorical and technological of view (4 - 5 - 6). The following table presents the main characteristics of the experiment :

RADIATION	λK_α Cr 2.29 Angs. (30 Kv, 25 mA) Back filtered by Vanadium
SPOT SIZE	Circle 1.5 mm diameter
GEOMETRY	Classical laboratory goniometer (automated) Ω geometry
Ψ ANGLES	+/-39.23 ; +/-33.21 ; +/-26.56 ; +/-18.43 ; 0
DETECTION	Position Sensitive Detector (PSD) Time for Ψ acquisition : about 60 sec.

Table 3 - X Ray stress measurement conditions

With such conditions, the dispersion of the points around the mean straight line was good and led to a calculated accuracy, for the stress (80 % confidence) of about ± 25 MPa. The main origine of the dispersion observed comes from the positioning of the sample. In case of sharp variations of ΔK (end of fracture) a displacement less than 1 mm may give a result 50 MPa higher or lower. As will be seen on figure 9, this happened at least once. Spot size of 1.5 mm diameter may thus be too large.

Local electrochemical polishing has been used to remove thin layers of material. We controlled the depth with a profilometer and a comparator. On the curves, the points have been drawn at the mean penetration depth below the initial surface. The polished zone is not always very flat, and this is the second origin of the dispersion in the results.

As we could not achieve, for time reasons, a complete line profile analysis, we controlled the work hardening of the material through the simple breadth of the {211} diffraction peak. As will be seen on the results, it is a very sensitive parameter with high accuracy ± 0.03 (°).

CRACK GROWTH ANALYSIS

Influence of load ratio R and load frequency f

The influence of load ratio on fatigue crack growth for two different test frequencies (f = 65 Hz and f = 7 Hz) in moist air environment (RH = 25 ± 5 %, T = 22°C) is shown in figures 1 and 2. With high frequency tests the so called R effect is observed (figure 1). The higher R ratio gives higher crack growth rate especially in low ΔK region. On the contrary if the loading frequency is decreased enough ($f = 7$ Hz in the present study) the crack growth rate is largely unaffected, at least above 2×10^{-9} m/c, and for a large range of R (from 0.1 to 0.7) the growth rates are not significantly different (figure 2).

The exponent m of the Paris law is $m = 2.8$ for $R = 0.7$ tests independently of the load-frequency. For the $R = 0.1$ tests the crack propagation law depends on the load-frequency : $m = 4.3$ for the high frequency test and $m = 3$ for the low frequency test.

It is generally accepted than the R ratio effect on fatigue crack growth is related to the crack closure phenomenon. For low ratio (i.e. $R = 0.1$ in this study) in the low ΔK range, before the load reaches its minimum, crack closure occurs (7). Therefore a portion of the cyclic loading is needed to open the crack and the effective load range available for the fatigue process is smaller than the applied load range. From crack closure measurement we can calculate the effective stress intensity factor ($\Delta K_{eff} = K_{max} - K_{op}$) and the opening ratio ($U = \Delta K_{eff}/\Delta K$) which is an indication of the amount of cl [illegible]

The frequency effect is far l [illegible] ce. This phenomenon observed by Y [illegible] Seif [illegible] is al[illegible] discu[illegible] rough the [illegible] l [illegible], fo[illegible] fre[illegible], that a thi[illegible] oxide is develop[illegible] th low R and [illegible] conditions) which enhances closure. T[illegible] layer is thinn[illegible] when the test f[illegible] is lower, at least below 10 Hz and for the test at frequenc[illegible] R = 0.1 no significant closure is detected [illegible] eferences 10 and 11).

SURFACE RESIDUAL STR[illegible] ON [illegible] CKED SURFACE

Measurements on the crack pla [illegible] and σ_T on figure 3.

The values of σ_L are systemat[illegible] wice higher than σ_T values (Fig. 4 and 5). For $R = 0.1$ tests, longitudinal residual stresses are of 250 MPa and transversal residual stresses are of 100 MPa. Both remain roughlt constant in the range $10 < \Delta K < 30$ MPa $\sqrt{m}$. In the case of the $R = 0.7$ tests, longitudinal residual stresses reach, in the low ΔK range, 500 MPa which is slightly lower than the yield stress. For increasing ΔK there is a sharp decrease in residual stress values which reach the level of 250 MPa at a ΔK of 30 MPa$\sqrt{m}$. The other information comes from the broadening of diffraction peaks. The half height chord breadth is reported in figure 6.

Compared to the nominal level which is about 1.90°, the half height chord breadth is a significantly higher for the high R ratio test than for the $R = 0.1$ test where no closure occurs. The test at high frequency and $R = 0.1$ shows a considerable broadening of diffraction peaks for the low ΔK range, which progressively disappeared to reach the nominal level for $\Delta K = 25$ MPa$\sqrt{m}$. On figure 7 the opening ratio $U = \Delta K_{eff}/\Delta K$ against ΔK measured during fatigue tests is plotted.

Comparing figures 6 and 7 it is obvious that closure, which only occurs for the $R = 0.1$ and high frequency test has a strong influence on surface X-Ray diffraction peak broadening. If we look at the results from the $R = 0.1$ tests, the evolution of closure and peak broadening follows the same trend. The

results from the high R ratio show higher peak breadth which slightly decreases with [illegible] sing ΔK.

The measurements on the [illegible] ite difficult to interprete because of the combined effects of closure, R ratio and stress intensity level. Tanaka and Hatano [illegible] (1) also show this complex behaviour of [illegible] udy [illegible], on constant ΔK fati[illegible] st, s[illegible] ese surface residual stresses might also depend on crack length.

[illegible] ASTIC ZONE SIZE [illegible]

More encouraging are in depth measurements of residual stresses and diffraction peak broadening after successive electrochemical polishing. From the in depth distribution of residual stres[illegible] breadths, the limit of the plastic zone is fixed at a depth where the original values (for the unstraine[illegible] results of stresses and hardening against the depth from the fracture surface are plotted on figures 8a and 8b.

Th[illegible] st estimation of the plastic zone limit is given by linear regression between the measured values and the square root of the depth. Such curves are given in figures 9a and 9b for specimen C.

The monotic plastic zones determined from these measurements are compared to an analytical solution in plane strain. The theoretical solution is calculated from the Westergaad equations of stresses :

$$\sigma_1 = \frac{K}{\sqrt{2\pi r}} . \cos\frac{\theta}{2} . (1 + \sin\frac{\theta}{2})$$

$$\sigma_2 = \frac{K}{\sqrt{2\pi r}} . \cos\frac{\theta}{2} . (1 - \sin\frac{\theta}{2})$$

$\sigma_3 = 0$ in plane stress

$\sigma_3 = \nu (\sigma_1 + \sigma_2) = 2\nu \frac{K}{\sqrt{2\pi r}} \cos\frac{\theta}{2}$ in plane strain

if the Tresca yield criteria is used, for plane strain condition :

$$\tau max = \frac{1}{2} (\sigma_1 - \sigma_3) \text{ or } \tau max = \frac{1}{2} (\sigma_1 - \sigma_2)$$

The limit of the plastic zone, in plane strain is given by the larger of :

$$r_p = \frac{1}{2\pi} \left(\frac{K_{max}}{\sigma_{ys}}\right)^2 . \cos^2\frac{\theta}{2} (1 - 2\nu + \sin\frac{\theta}{2})^2$$

or

$$r_p = \frac{1}{2\pi}\left(\frac{K_{max}}{\sigma_{ys}}\right)^2 . \left(2 \cos \frac{\theta}{2} . \sin \frac{\theta}{2}\right)^2$$

for $\theta = 90°$ $r_p = 0.159\left(\frac{K_{max}}{\sigma_{ys}}\right)^2$

Analytical and experimental results compared on figures 10a and 10b are quite encouraging.

A better correlation is obtained by the estimation of plastic zone size from peak breadth value. This is supported by the fact that peak breadth is only affected by the plastic deformation within the plastic zone, after unloading the plastic zone is too large for its elastic surroundings. Then the elastic material has to make it fit, and elastic residual stresses are encountered outside of the plastic zone.

Refering to figure 8b, the in depth peak breadth distribution shows, when no closure occurs, are interesting profile. The peak breadth reaches its maximum slightly under the fracture surface. This maximum value is found deeper for the higher ΔK values whatever the R ratio is. We should note that in the case of specimens B and C, the depth corresponding to the maximum peak breadth is roughly at the same magnitude than the cyclic plastic zone calculation as

$$r_{pc} = 0.159\left(\frac{\Delta K}{2\sigma'_{ys}}\right)^2$$

where σ'_{ys} is the cyclic yield strength.

CONCLUSION

Encouraging results are obtained with the X-Ray fractography technique especially in determination of plastic zone size as small as 50 μm and in plane strain condition, where usual experimental techniques are limited.

Surface measurements are found difficult to interprete due to the numerous varying parameters such as crack closure, surface roughness, crack length, R ratio, stress intensity level...

More interesting are the in depth measurements of stresses and X-Ray diffraction peak breadth. This method was used in the study, very successfully, to determine the fatigue crack plastic zone size. Distribution of in depth residual stresses is found to be proportional to the square root of the depth from the fracture surface, and plastic zone size limits correspond to the depth where residual stresses become null.

Useful information is also provided by the X-Ray diffraction peak breadth distribution. The peak breadth goes from the very crack surface, from low values to reach a maximum which depends upon ΔK and probably corresponds to the cyclic plastic zone limit, then decreases towards the initial value (for unstrained material) which is found to be reached at the monotonic plastic zone limit.

Comparison between experimentally determined plastic zone size and analytical solution shows a rather good agreement especially by using the peak breadth measurements.

REFERENCES

1) K. Tanaka and N. Hatanaka, (1982), J.S.M.S. Vol 31 p. 215

2) Y. Kurebayashi, S. Kodama, H. Misawa, (1982) J.S.M.S. Vol 31 p. 221

3) M. Kikuwa, M. Jono, K. Tanaka and M. Takatai, (1977), J. of Mat. Sci. Vol 26 p. 1964

4) L. Castex, J.L. Lebrun, G. Maeder, J.M. Sprauel, (1981), Pub. Sci. et Tech. ENSAM n° 22

5) H.T.M. Beiheft 82 Eigenspannungen 1982

6) G. Maeder, J.L. Lebrun, J.M. Sprauel - Present possibilities for X-Ray diffraction method of stress measurements - (1981), N.D.T. International p. 234 - 247

7) W. Elber, (1971), ASTM STP 486 p. 230

8) T. Yokobori and K. Sato, (1976), Eng. Fract. Mech. Vol 8 p. 81

9) H.G. Noack and K. Seifert, (1980), "Analytical and Experimental Fracture Mechanics", Proc. Int. Conf. Rome - June 1980 G.C. Sih ed., Sijthoff and Noordhoof

10) A. Bignonnet, R. Namdar-Irani and M. Truchon, (1982), Scripta Met. Vol 16 p. 795

11) A. Bignonnet, R. Namdar-Irani and M. Truchon, (1982), "Fracture and the role of microstructure" Proc. of the 4th E.C.F. Leoben-Austria 22-24 Sept. 1982, K.L. Maurer and F.E. Matzer, eds. EMAS, pp. 417 - 425

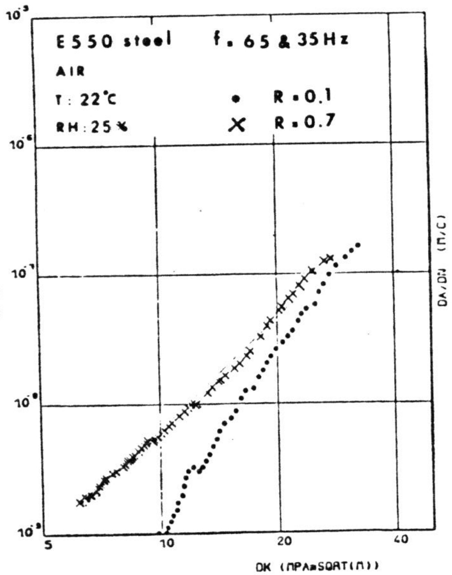

Fig. 1 - Fatigue crack growth rate at high frequency for the 2 R ratios

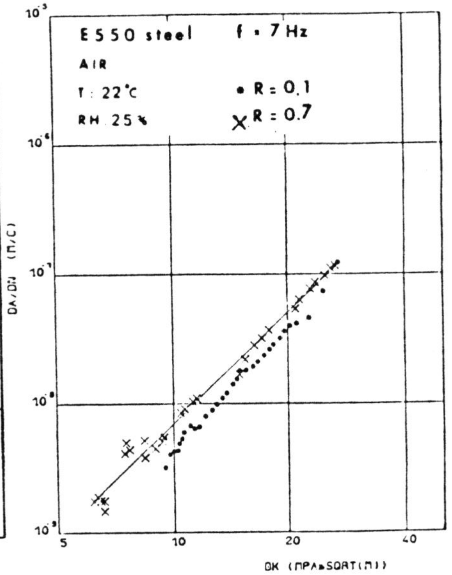

Fig. 2 - Fatigue crack growth rate at low frequency for the 2 R ratios

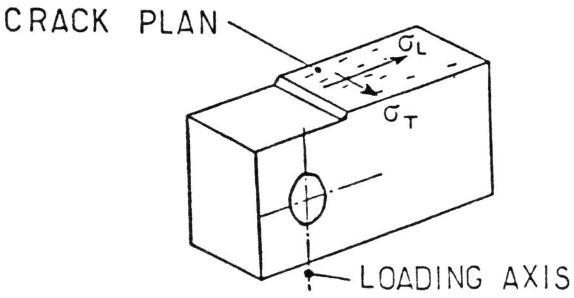

Fig. 3 - Orientation of the measured stresses

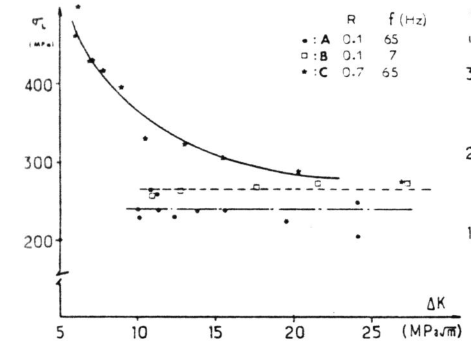

Fig. 4 - Surface longitudinal stresses against ΔK

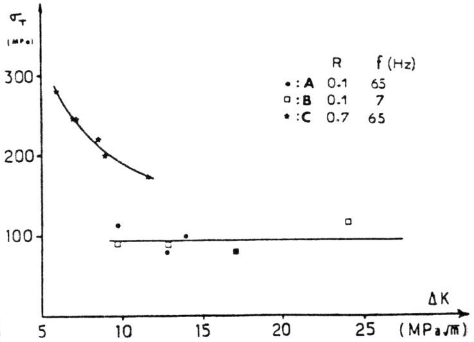

Fig. 5 - Surface transversal stresses against ΔK

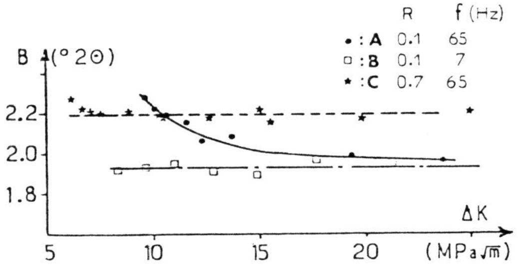

Fig. 6 - Surface peak breadth against ΔK

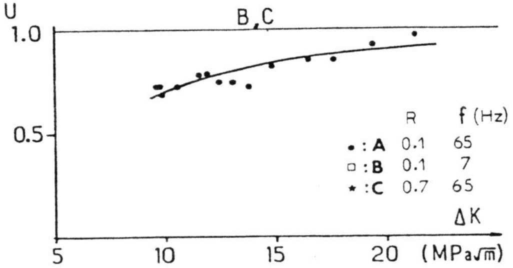

Fig. 7 - Opening ratio U against ΔK

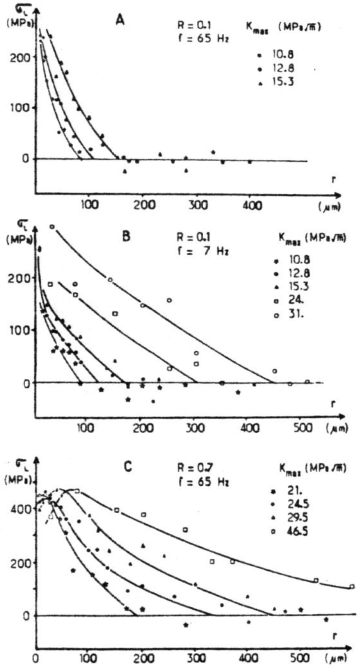

Fig. 8a - In depth longitudinal stresses measurements

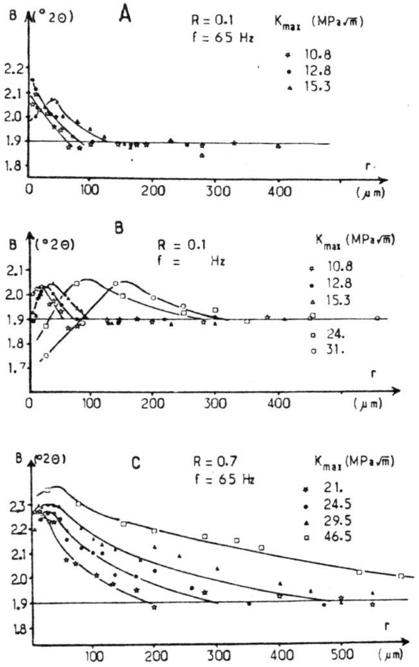

Fig. 8b - In depth peak breadth measurements

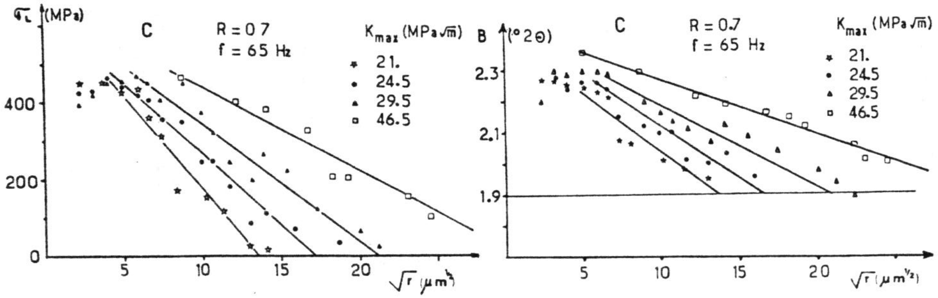

a)

b)

Fig. 9 - Distribution of the a) longitudinal stresses b) the peak breadth against square root of depth

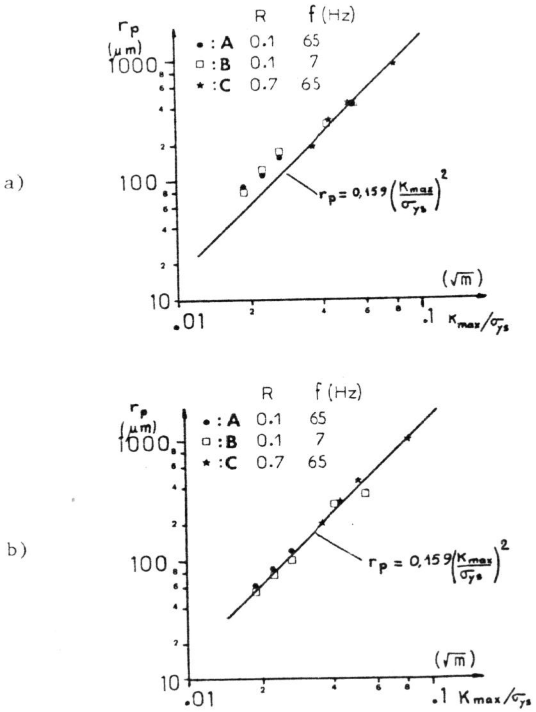

Fig. 10 - Comparison between analytical solution and estimated plastic zone size for a) stresses and b) peak breadth measurements